

ASTER IMAGERY AND AEROMAGNETIC DATA - POWERFUL TOOLS TO AID RECONNAISSANCE GEOLOGIC MAPPING OF THE SIERRA SAN JOSÉ MOUNTAIN RANGE, NORTHERN SONORA STATE, MEXICO

*J.C. Wynn, US Geological Survey, Vancouver, WA
J.L. Mars, US Geological Survey, Reston, VA
Floyd Gray, US Geological Survey, Tucson, AZ
A.P. Schultz, US Geological Survey, Reston, VA
F.A. Maldonado, US Geological Survey, Denver, CO
F.A. Villaseñor, SEMARNAT, Cananea, Sonora, Mexico
L.M. Brady-Norman, US Geological Survey, Tucson, AZ*

Abstract

Aeromagnetic and Advanced Spaceborne Thermal Emission and Reflection Radiometer (ASTER) data are currently being used to assist in geologic mapping of the Sierra San José region in the Sonoran San Pedro River basin. Lithologic contacts have also been mapped using Euler deconvolution of aeromagnetic data. A lithologic classification map consisting of quartz-feldspar, clay-muscovite-sericite, and carbonate was produced using thresholded match filter ASTER data and relative band depth absorption analysis (RBD). A minimum noise transform (MNF) false color composite image was used to map lithologic units. A false color composite image of ASTER bands 1 (blue), 2 (green) and 3 (red) was also used to determine the extent of vegetation and assist in mapping structural features, although most of the structural features could be mapped using high altitude stereo pair imagery. To date, field studies indicate that ASTER data have successfully mapped carbonates, sericite, and muscovite and with lesser success have also helped characterize quartz-rich rocks. In addition, our field studies, along with ASTER and Landsat data, have confirmed lithologic contacts at the surface mapped by Euler deconvolution of the aeromag.

Introduction

The San Pedro River drainage straddles the border between Arizona and Sonora, Mexico. As part of a larger cooperative study of water and mineral resources in the US-Mexican Borderlands region, the USGS and SEMARNAT (the Mexican Environmental and Natural Resources Agency) have undertaken a detailed joint study of the Sonoran San Pedro River basin. This work is designed to supplement earlier geologic maps and a previous analysis of the ground water resources on the American side of the frontier. Within the Sonoran San Pedro drainage lies the Sierra San José, an eight-by-fifteen-km mountain range that has apparently not been previously geologically mapped in any detail. Geologic mapping of the region is critical due to the unusual position of the Sierra San José within the San Pedro drainage, and some suggestion from geophysical data that there are possible hidden structures constraining groundwater flow in the water-saturated sediments to the south, west, and north of the mountain.

The Sierra San José has a maximum elevation of approximately 2,500 meters and is surrounded by the San Pedro plains at an average elevation of 1,500 meters. It is substantially covered with vegetation, especially at higher elevations, and is extremely rugged. In order to maximize the efficiency of our mapping team and minimize the risk of injury, satellite imagery and airborne geophysical data were collected prior to geologic field mapping. These data were used to develop a preliminary working map of the mountain. Geology in the nearby Mule Mountains and Coronado National Monument on the American side of the border was researched and augmented with Landsat TM imagery. Helicopter-acquired magnetic data over the Sierra San José acquired from the Cyprus mining company (now part of Phelps-Dodge Corp.) was processed and used to map magnetic gradients, which are potential geologic contacts. These contacts as well as domains derived from the Landsat imagery were then superimposed on a topographic base map generated from Mexican digital elevation models. The most useful tool for geologic mapping, however, was Advanced Spaceborne Thermal Emission and Reflection Radiometer (ASTER) imagery. Ultimately, we depended on several different processed ASTER images and a gradient map of the aeromagnetic data to develop our first working field map of the Sierra San José.

Background

The San Pedro River originates in northern Sonora State in Mexico, and extends into southeastern Arizona, where it ultimately joins the Gila River (figure 1). During most of its course, its surface water is critical to a major North American (US, Mexico, Guatemala, etc.) migratory bird flyway. As part of a US Army-supported effort to understand the San Pedro River and its supporting aquifer, the US Geological Survey carried out airborne geophysical surveys on the American side of the international frontier (Wynn and others, 2000; Wynn, 2000/2003). Because the San Pedro basin extends almost 50 kilometers into Mexico, it is unreasonable to think that the groundwater regime could be adequately understood without information from the Mexican side. As part of a cooperative effort between the US Geological Survey and the Mexican Secretaria del Ambiente y Recursos Naturales (SEMARNAT) to understand the entire basin, joint mapping was begun on the Mexican side of the frontier in 2000. Early on it was realized that the Sierra San José, a roughly 8-km by 15-km, west-northwest-trending mountain range lying just south of the border near Naco, Sonora, had to figure prominently in the evolution of the sedimentary basin on both sides of the border (see figure 2, derived from Dohrenwend and others, 2000). To our amazement, there were apparently no geologic maps of the mountain, and it became clear that we would have to complete at least a reconnaissance map in order to complete our basin study. Because we had limited time and resources, we turned to space-borne imagery to assist us. ASTER imagery, and to a lesser extent airborne magnetic data, became the critical resources we used in developing our initial reconnaissance “pseudo-geology” maps to guide our field follow-up. Because this is a work in progress, only a few examples of the new geologic information will be shown in this paper.

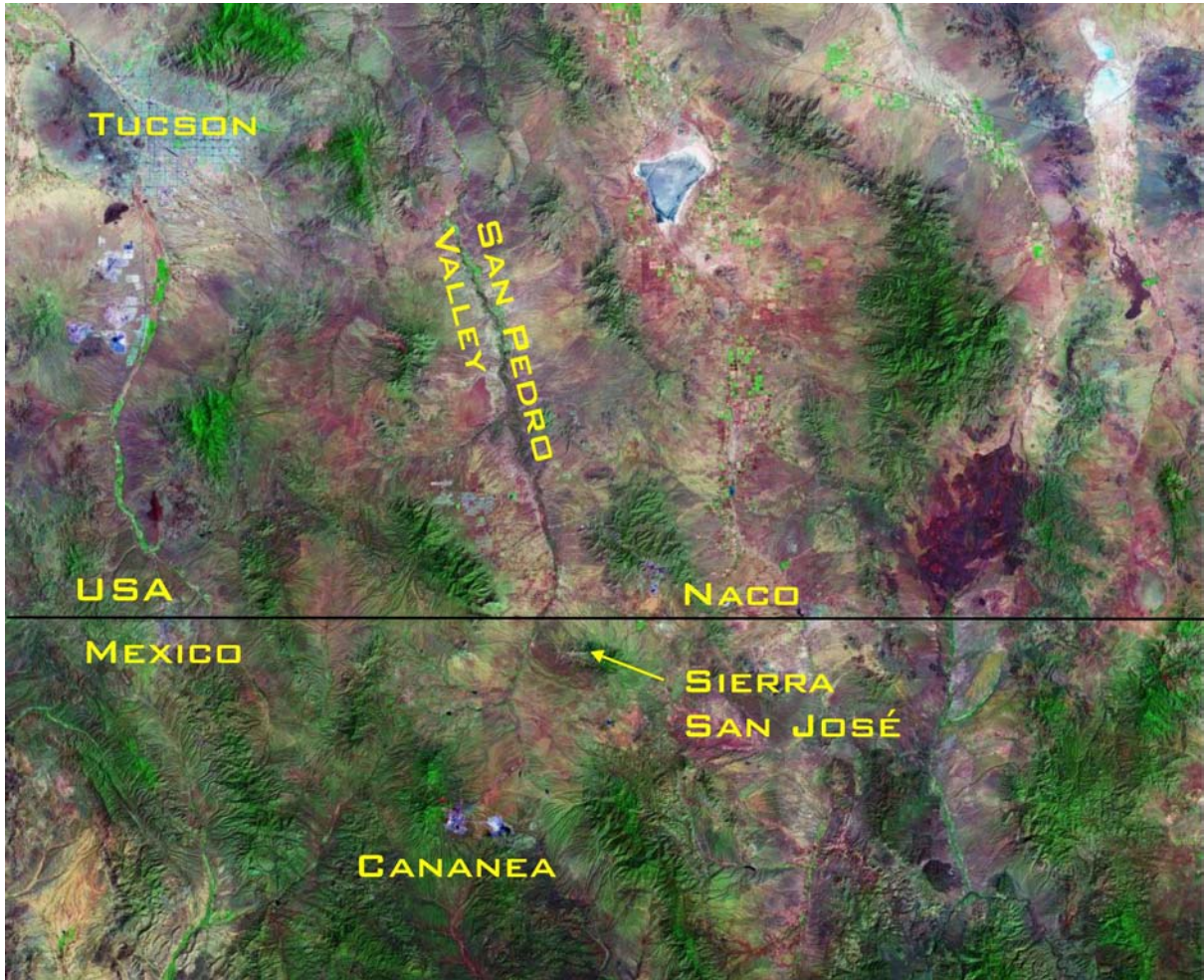


Figure 1. Index map showing the Sierra San Jose mountain range in northern Sonora State, Mexico

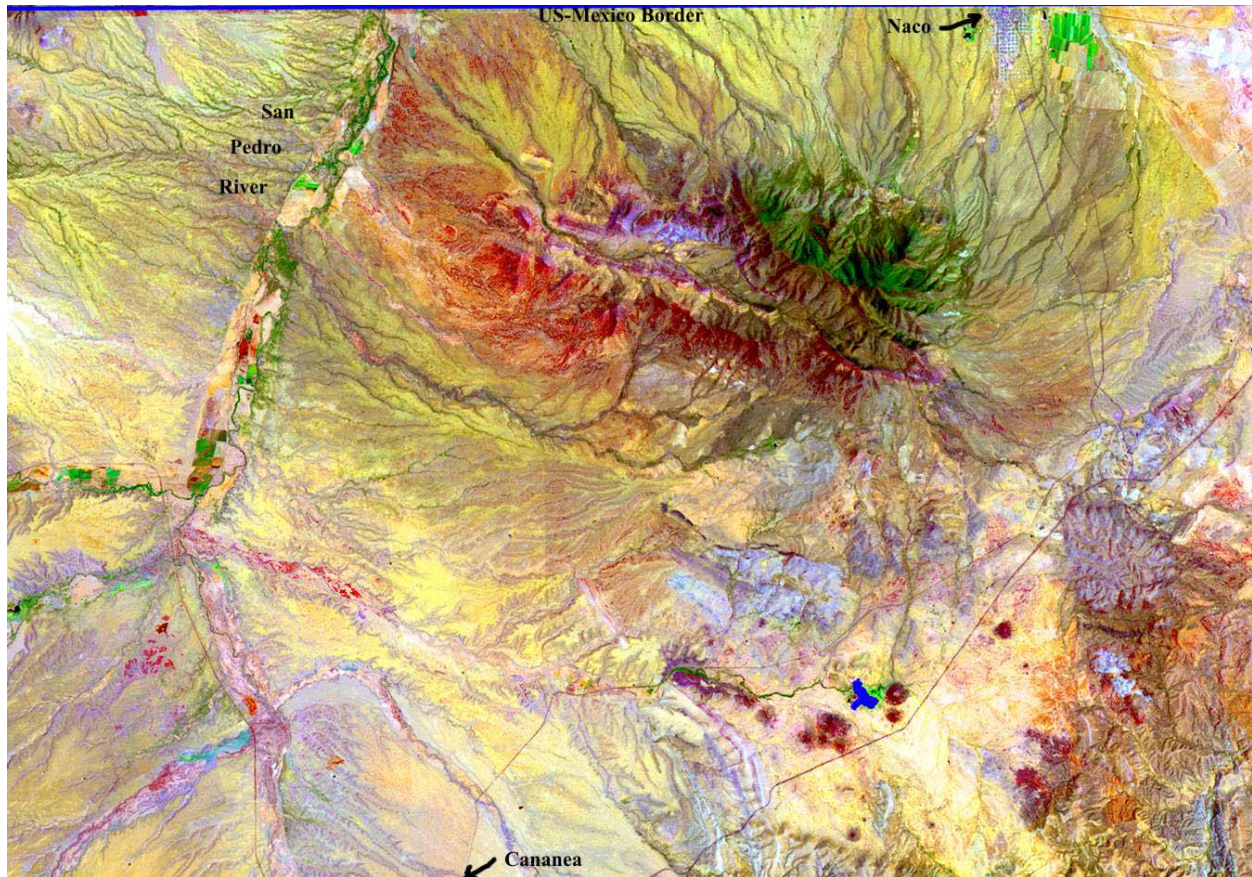


Figure 2. A LANDSAT image of the Sierra San Jose, northern Sonora State, Mexico. The Sierra is the large colored object in the top center. The towns of Naco, Arizona, and Cananea, Sonora are indicated.

Euler Deconvolution and Geologic Contacts

Euler deconvolution is used to calculate depth-to-source information from airborne magnetic data (for an explanation of how this derivative product is obtained, see Blakely, 1995). The deconvolution process depends upon inflections or changes in the magnetic field, and pinpointing those inflections (which imply subtle variations on magnetite content of the underlying rock) generally identifies geologic contacts. Figure 3 shows the unwinded Euler deconvolution solution-points overlaid on a color-scaled, shaded digital elevation map of the Sierra San José. These Euler solutions use different window-widths as they pass over the gridded magnetic data, and different windows often give rise to slightly different solution-points for non-vertical contacts. These “dispersed” contacts, some of which can be seen in the figure, could be caused either by a gradational change in magnetite content in the underlying rocks (a facies change in sedimentary rocks, for instance) or by a dipping fault or contact. In either case, the distribution of solution-points provides information on subsurface structure: where the geologic contact is, and whether it is vertical, dipping, or gradational. On the exposed rocks of

the Sierra San José itself, the solution-point contacts can generally be correlated with contrasts in the Landsat or ASTER imagery, or with exposed faults and contacts that we were later able to verify in the field. On the periphery of the Sierra these solution-point contacts can be inferred to map geologic contacts in crystalline rock underlying the Quaternary alluvium and older basin-fill.

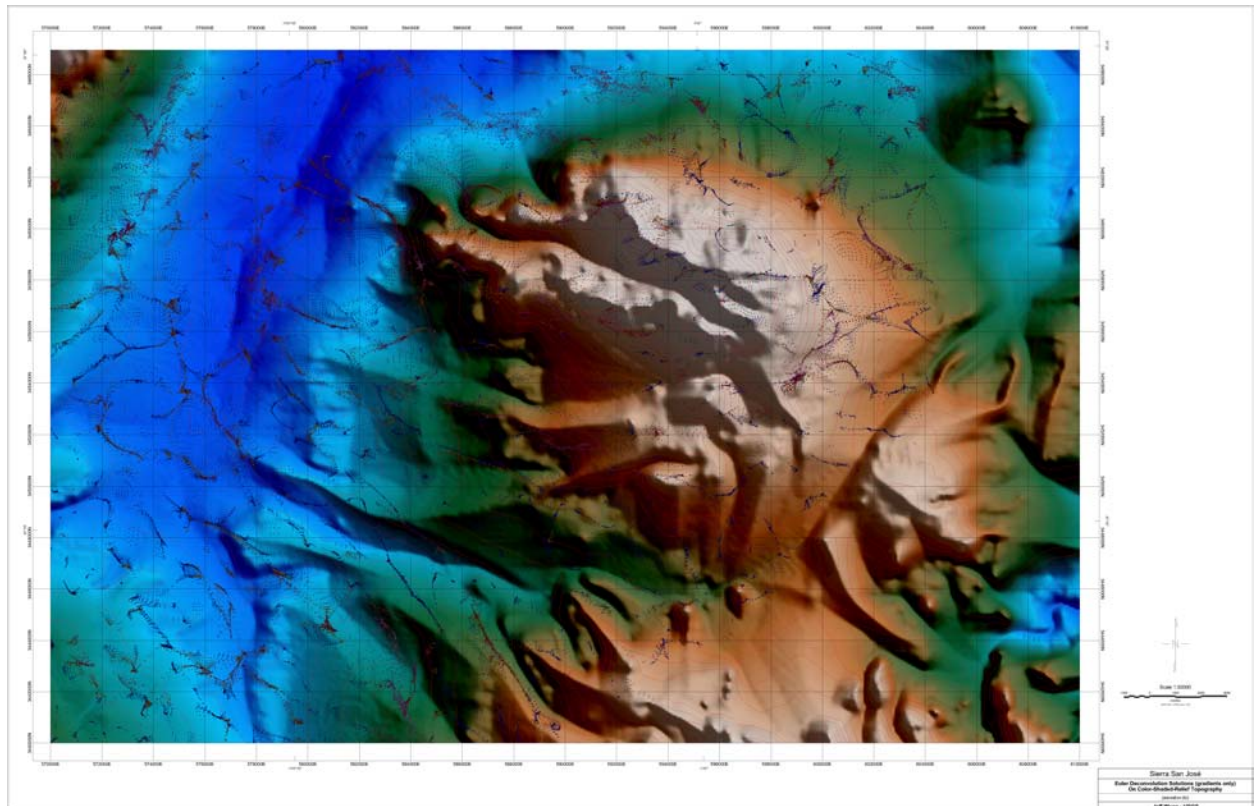


Figure 3. Euler Deconvolution solutions (small black dots) from aeromagnetic data, superimposed on a colored, shaded relief map of the Sierra San Jose.

ASTER Imagery

ASTER data consists of three 15-meter, six 30-meter, and five 90-meter resolution bands in the 0.52 to 0.86, 1.65 to 2.43, and 8.13 to 11.65 micrometer region, respectively. NASA and the Japanese Space Agency jointly acquired these data. ASTER data (radiance level 1b) were obtained from the Earth Remote Sensing Data Analysis Center (ERSDAC) and converted to reflectance data using Modtran 4 atmospheric correction software. The ASTER dataset extended from the study area in Mexico to the American side of the border, where published geologic maps exist. We calibrated the ASTER imagery against geologic maps by Drewes (1980, 1996), Moore (1993), DuBray and others (1996), and Kneale and others (1997).

A map and two images were produced from 9 bands of ASTER data (0.52 to 2.42 micrometer region) to map the study area. A classification map was used to map mineralogy (Fig. 4), a false color composite map of ASTER bands 3, 2, and 1 was used to delineate quartz and feldspar rich rocks and to map structure (Fig. 5), and a false color composite MNF image was used to map lithologies (Fig. 6). Three ASTER bands in the 0.52 to 0.86 micrometer region are positioned to map the Fe^{3+} absorption feature and five of the ASTER bands are positioned in the wavelength region between 2.1 and 2.4 micrometers in order to measure reflectance of Al-O-H, Mg-O-H, CO_3 , and Si-O-H absorption features.

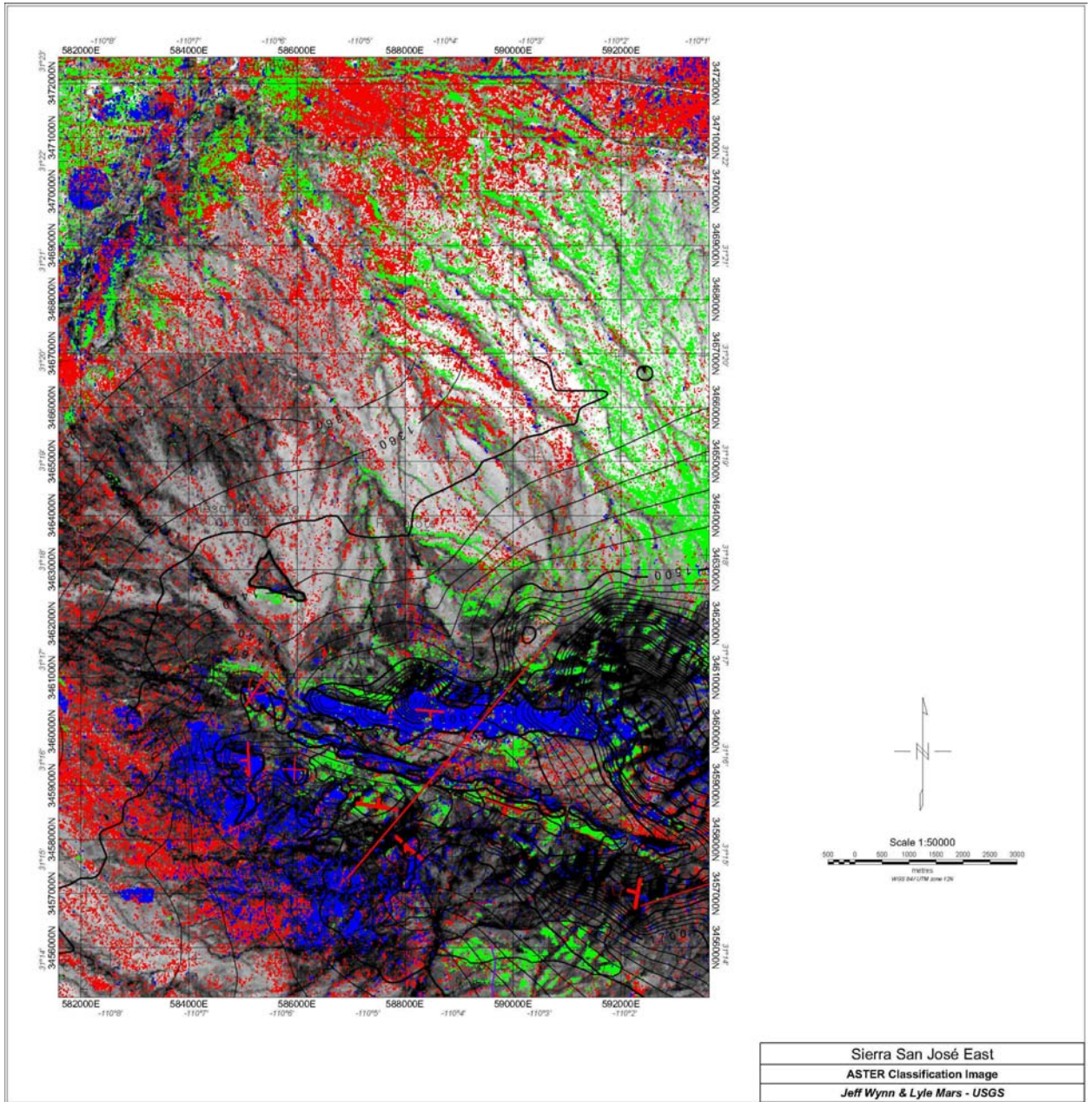


Figure 4. Classification map using ASTER imagery, Sierra San Jose. Red represents quartz, green represents clay, and blue represents carbonate in this image. Structure is shown as red lines, topo contours are black.

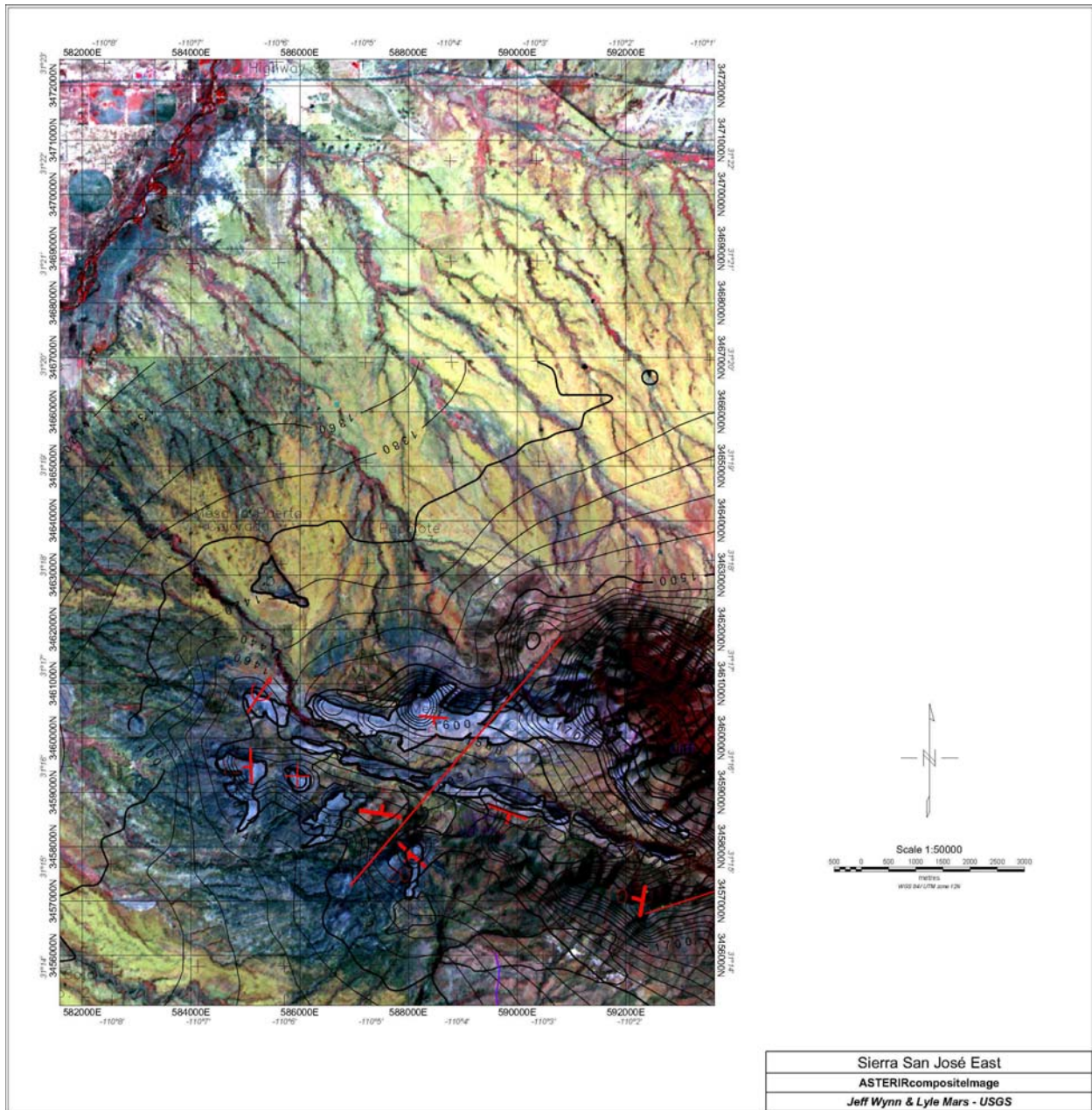


Figure 5. Infra-red composite image from ASTER imagery, Sierra San Jose. Same colors for lines as fig. 4.

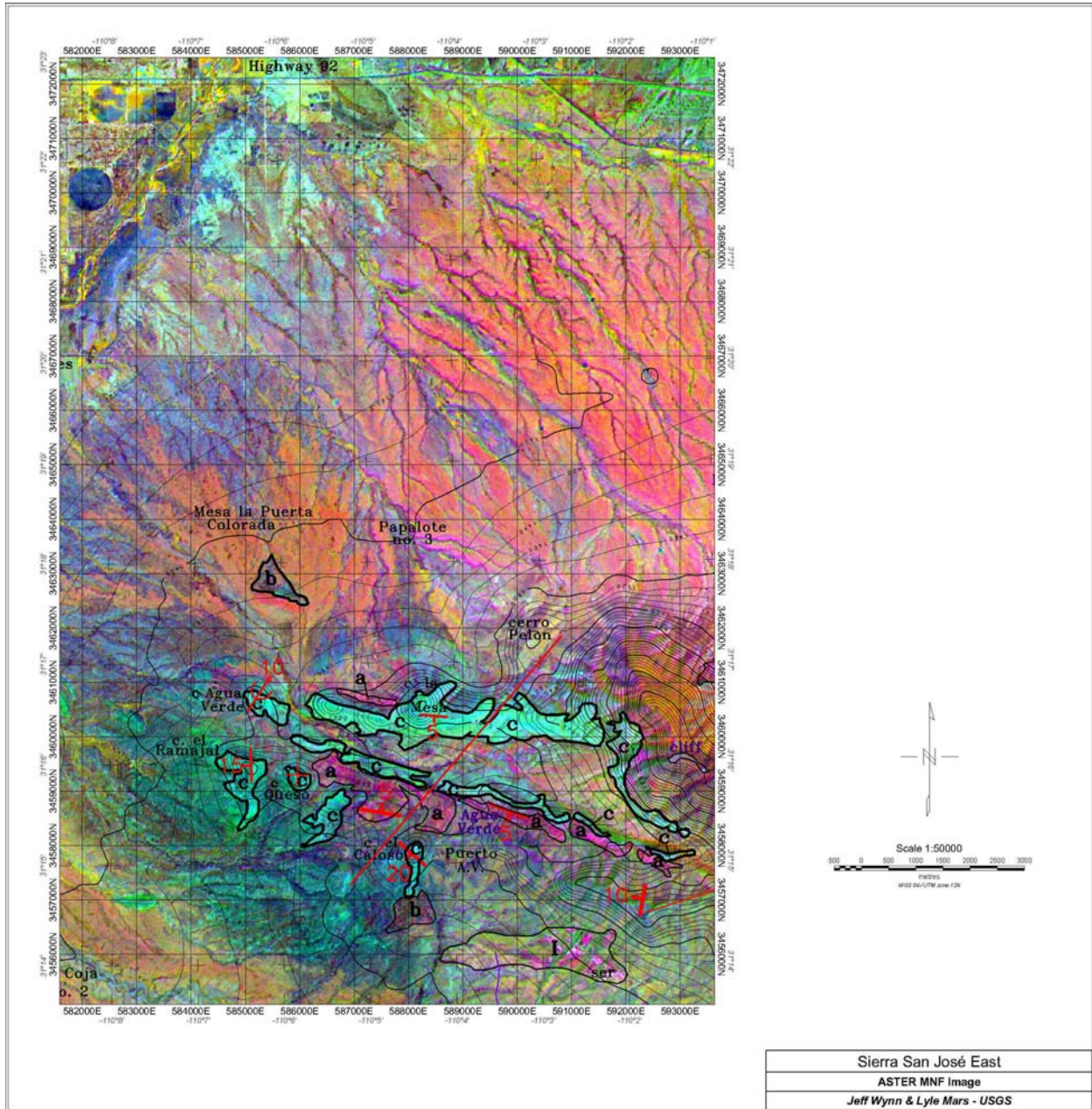


Figure 6. Minimum Noise Transform derived from ASTER imagery, Sierra San Jose. Line colors as in fig. 4.

Relative band depth (RBD) and matched filter analysis were used to produce the ASTER minerals classification map. RBD images are generated by adding together bands of the shoulders of an absorption feature and then dividing these by the absorption feature minimum band (Rowan and Mars, in press). Thus, pixels with high digital number values in RBD images illustrate the most intense absorption feature. RBD images were thresholded, and spectra were

extracted and used as endmember spectra in matched filter analysis. The matched filter algorithm is designed to use image spectra and can partially unmix pixels that contain multiple spectral features (Boardman and others, 1995). Thus, the matched filter algorithm typically produces an image that is more accurate than an RBD image. The matched filter images were thresholded and used to produce the mineralogical classification map. Carbonate, as well as sericitic alteration, muscovite, and clay, were mapped using the 2.33 (band 8) and 2.2 (band 6) micrometer absorption features, respectively (Figure 4, Blue and Green, respectively).

Rocks rich in quartz and feldspar were mapped by examining a false color composite image of ASTER bands 3 (red), 2 (green) and 1 (blue) (Fig. 5). Quartz and feldspar rich rocks typically appear white in the RGB 3, 2, 1 image and have featureless spectra with high reflectance values. The featureless spectra with the highest reflectance values were extracted and averaged to produce a spectral endmember that was used in matched filtering to produce a quartz – feldspar image. The quartz –feldspar image was thresholded to produce the quartz-feldspar unit in the classification map (Figure 6, Red).

A Minimum Noise Transform (MNF) image was used to identify the maximum number of lithologic units from ASTER data in a single false color composite image (Fig. 4). The MNF algorithm consists of a double cascade principal component analysis designed to separate noise from useful spectral units such as specific rock types and vegetation (Green and others, 1988). The match filter images and mineral classification map were used to identify the MNF bands that contained the most lithologic spectral units. The MNF analysis of 9 ASTER bands (0.52 to 2.43 micrometer region) compressed most of the lithologic spectral units into MNF bands 3 through 5. MNF bands 1 and 2 contain mostly vegetation and shadow spectral units, and bands 6 through 9 contain mostly noise. In the upper left corner of the MNF false color composite image (MNF band 3= red, MNF band 4= green, MNF band 5=blue), several crop circles can be seen (Fig 4). The red colors in the MNF image are alluvial fan deposits from the northwest parts of the Sierra San José. The teal-colored units (labeled “c”) are limestone-capped sedimentary rocks, the red units (labeled “a”) are underlying quartz-rich sandstone, and the brown unit (labeled “b”) is a quartzite body. The classification map incorrectly mapped unit “a” as a clay-rich unit. Image spectra from unit “a” contain a 2.2 micrometer absorption feature typical of clay-rich rocks. Further spectral analysis of unit “a” samples is therefore needed. Structure information on the map (red lines) is derived from limited field visits and the extensive use of ground-based stereo-photo pairs taken in the field. On this image tentative contacts are outlined in thick black lines, and topography (20-meter intervals) is shown with thin black lines. The unit labeled “I” is discussed below.

The 15 m resolution visible near-infrared bands 1, 2, and 3 were combined in an ASTER infrared composite image (band 3= red, band 2= green, band 1=blue) in order to illustrate the extent of vegetation cover (Fig. 5, red pixels in the image), and to delineate any structural features. This is the highest spatial resolution RGB image possible using ASTER data. On top

of this image is superimposed the same tentative geologic contacts derived from the MNF image. This image shows more detail in the alluvial fan, but also shows dark stippling caused by vegetation. In general there is less information about underlying rock types available in this image.

Figure 7 is a close-up of the MNF image of figure 4, showing the GPS track (blue line) of our field sampling traverse. Sample stations are labeled in black in this image. Before we arrived in the field, our ASTER specialist (JCM) had characterized the “I” unit (for intrusive) in this image as probably a granite body from its spectral characteristics. As we approached the unit from the north we saw increasingly-steep dipping beds in the surrounding sedimentary units, reaching 80°N dip just before we encountered the intrusive unit, which proved to be a coarse-grained granite. On the east edge of the intrusive there are several pixels in the ASTER imagery that are suggestive of sericite alteration, something not unexpected at an intrusive-sediment contact.

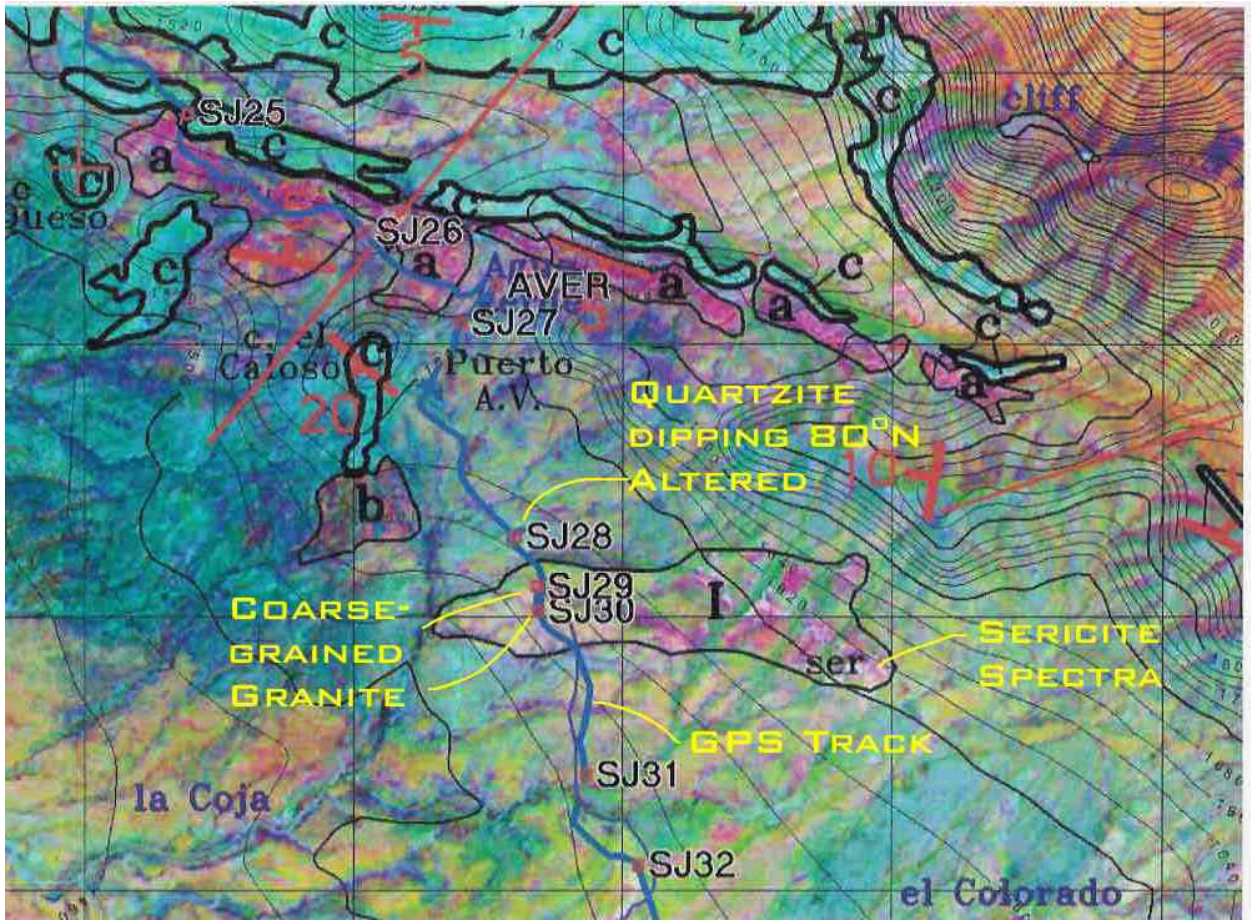


Figure 7. A close-up part of figure 6, the Minimum Noise Transform image, for the south side of the Sierra San Jose

Conclusions

We have completed only our first field season on the Sierra San José, after only about 10 days on the ground. We feel we have some unusually powerful tools at our disposal, tools that have dramatically increased our mapping efficiency in this rugged, almost inaccessible mountain range in northern Mexico. The Euler deconvolution solution-sets, irrespective of the depth-to-source information they provide, also give 3-D structural information. ASTER imagery successfully identified and mapped carbonates, and sericite/clay-altered rocks, and was somewhat less successful in mapping quartz-rich rocks. The quartzite unit mapped as clay or muscovite-rich rock will be evaluated using field samples and ASTER thermal data. Carbonates from the nearby Bisbee Group have slightly different spectral characteristics from carbonates that we field checked at Sierra San José. The differences appear to be due to age - Paleozoic vs. Cretaceous Bisbee Group. The altered rocks mapped by ASTER helped delineate several intrusive rock units later found and verified during field mapping. These intrusives are found on both north and south sides of the Sierra, and presumably have given rise to the substantial (at least 1,000 meters) apparent vertical uplift we observed in the eastern part of the mountain. Finally, in areas not easily accessible, digital stereo-pair photo imagery was used to map sedimentary and other large-scale structures in three dimensions, thus substantially augmenting details observed on the ground. The result is a reconnaissance geologic map with a degree of detail (and confidence) that belies the limited resources available to us in our first short field season. It also provides us a strong base upon which we plan to build our final map of the Sierra San José.

References

1. Blakeley, R.J., 1995, Potential theory in gravity & magnetic applications: Cambridge University Press, New York, 441 p.
2. Boardman, J.W., Kruse, F. A., and R.O. Green, 1995, Mapping target signatures via partial unmixing of AVIRIS data, in Proceedings of the Fifth JPL Airborne Earth Science Workshop, JPL Publ. 95-01, p. 23-26, Jet Propul. Lab., Pasadena, Calif.
3. Dohrenwend, J.C., Gray, Floyd, and Miller, Robert J., 2001, Processed Landsat Thematic Mapper satellite imagery for selected areas within the U.S. - Mexico borderlands (false color composite image, Path 35 Row 38; acquired on 24 June 1997, (band 7 - red; band 4 - green; band 2 - blue):US Geological Survey Open-File Report 00-309, Version 1.0, 2001, three CD-ROMs.
4. Drewes, Harald, 1980, Tectonic map of southeast Arizona: U.S. Geological Survey Miscellaneous Investigations Series Map I-1109, scale 1:125,000.
5. Drewes, Harald, 1996, Geologic maps of the Coronado National Forest, southeast Arizona and

southwest New Mexico: U.S. Geological Survey Bulletin 2083-B, pp. 17-41, plates 2-4.

6. DuBray, E.A., ed., 1996, Mineral resource potential and geology of Coronado National Forest, Southeastern Arizona and Southwestern New Mexico, U.S. Geological Survey Bulletin 2083-D.

7. Green, A.A., Berman, M., Switzer, B. and M.D. Craig, 1988, A transformation for ordering multispectral data in terms of image quality with implications for noise removal, IEEE Trans. Geosci. Remote Sens., 26(1), 65-74

8. Kneale, Sean; Bultman, Mark; Chan, Tammy; Grisolano, Anna; and Hirschberg, Doug, 1997, Coronado National Forest Geology: unpublished Administrative report to the U.S. Forest Service, Coronado National Forest (CD-ROM).

9. Moore, R.B., 1993, Geologic map of the Tombstone volcanic center, Cochise County, Arizona: U.S. Geological Survey Miscellaneous Investigations Series Map I-2420, scale 1:50,000

10. Pool, D.R., and Coes, A.L., 1999, Hydrogeologic investigations of the Sierra Vista subbasin of the Upper San Pedro River Basin, Cochise County, Arizona: US Geological Survey Water-Resources Investigations Report WRIR 99-4197, 47 p., 3 plates.

11. Rowan, L. C., and Mars, J. C., in press, Lithologic mapping in the Mountain Pass, California area using Advanced Spaceborne Emission and Reflection Radiometer (ASTER) data: Remote Sens. Environ.

12. Wynn, J.C., 2000/2003, Mapping Groundwater in Three Dimensions: An Analysis of the Airborne Geophysical Surveys of the Upper San Pedro River Basin, Cochise County, Southeastern Arizona, with an Interpretation of the Water-Bearing Characteristics of the Underlying Geologic Units: US Geological Survey Open-File Report 00-517, 45 pages, 2 plates. [*Also: US Geological Survey Digital Professional Paper DPP-XXX*].

13. Wynn, Jeff, with Don Pool, Mark Bultman, and Mark Gettings, and Jean Lemieux, 2000, Airborne EM as a 3-D aquifer-mapping tool: Proceedings Volume, SAGEEP-2000 Conference, 20-24 February 2000, Arlington, VA., pp. 93-100.

14. Wynn, J.C., 2001, Cananea magnetic data processing, northern Sonora State, Mexico: US Geological Survey Administrative Report, 4 pages, 5 figures, plus gridded data (CD-ROM).

15. Wynn, Jeff, 2002, Evaluating ground water in arid lands using airborne magnetic and airborne electromagnetic methods - an example in the southwestern U.S. and northern Mexico: *The Leading Edge*, Vol. 20, no. 12 (January 2002 issue), pp. 62-65.